Head Taper Corrosion Causing Head Bottoming Out and Consecutive Gross Stem Taper Failure in Total Hip Arthroplasty

Michael M Morlock[1], Emilie C Dickinson[1], Klaus-Peter Günther[2], Dennis Bünte[3], Valerie Polster[1]
[1]TUHH Hamburg University of Technology, Hamburg, Germany;
[2]University Hospital Carl Gustav Carus, Dresden, Germany;
[3]University Hospital, Freiburg, Germany

Corresponding Author:
Michael M. Morlock
Institute of Biomechanics
TUHH Hamburg University of Technology
Denickestrasse 15
21073 Hamburg, Germany
morlock@tuhh.de
ph: +49 40 42878 3053
www.tu-harburg.de/bim

Abstract (250 words)

Head Taper Corrosion Causing Head Bottoming Out and Consecutive Gross Stem Taper Failure in Total Hip Arthroplasty

Background

Taper corrosion in Total Hip Arthroplasty for bearings with metal heads against polyethylene has developed from an anecdotal observation to a clinical problem. Increased taper wear and even gross taper failure have been reported for one particular design. It is hypothesized that corrosion of the female head taper results in taper widening, allowing the CoCr head to turn on the stem and wear down the softer titanium alloy by abrasive wear, ultimately causing failure. The purpose of this study was to investigate the time course of this process and the general role of taper dimensions and material in this problem.

Methods

Retrieved CoCr-alloy heads (n=30, LFIT, Stryker) and TMZF stems (n=10, Accolade I, Stryker) were available for analysis. Taper material loss was determined using 3D-coordinate measurements and scanning. The pristine tip clearance between head and stem was analytically determined. The influence of taper material and taper size on taper deformation and micromotion was investigated using a Finite Element Model.

Results

Material loss at the head taper increased with time in situ up to a volume of 20.8 mm^3 ($p<0.001$). A mean linear material loss above 76 µm at the head taper was analytically confirmed to result in bottoming out, which was observed in 12 heads. The FE calculations showed significantly larger deformations and micromotions for a small 11/13 TMZF taper combined with a distinctly different micromotion pattern compared to other materials and taper designs.

Conclusion

A 11/13 TMZF taper design with 36mm head diameters bears a higher risk for corrosion than larger tapers made from stiffer materials. Failures of this combination are not restricted to the head sizes included in the recall. Patients with this implant combination should be closely monitored.

Keywords: Taper corrosion, Gross Taper Failure, TMZF, Head Size

Introduction

Taper corrosion in Total Hip Arthroplasty (THA) has surfaced as a clinically relevant problem following the introduction of large head metal-on-metal (MoM) bearing articulations [1]. Recently it has also been more often reported for metal heads against polyethylene (PE) on a variety of stem designs [2;3]. It is widely acknowledged that any modular connection between metal alloys can exhibit corrosion problems if in contact with body fluids and exposed to micromotion [4;5]. The magnitude of micromotion during in-vivo loading is mainly influenced by 3 factors: the taper design and material [6], the assembly condition [7], and the loading magnitude and direction [8]. It was shown early on that low neck stiffness is a contributing factor [4]. It also has been shown that the changes in taper design in the last 20 years have led to more flexible tapers [6].

Several studies on elevated metal ion levels or even catastrophic gross taper failures (GTF) after hip joint replacement highlight one particular stem design with a small V-40 taper made from a less stiff Ti-12Mo-6Zr-2Fe titanium-alloy (TMZF; Accolade I, Stryker, Mahwah, NJ) in combination with head sizes of mostly 36mm and above (Figure 1) [9-18]. This proprietary beta titanium alloy was introduced in 2002 based on the potential benefits of more closely mimicking the modulus of elasticity of cortical bone than standard Ti-6Al-4V alloys [19]. The overall magnitude of the problem is unclear, with the number of cases reported in the literature being above 100 (including the cases reported in this study). In August 2016, the manufacturer issued a voluntary medical device recall for certain cobalt-chromium alloy (CoCr) head diameters (36mm and larger) in combination with certain offsets (+4mm. +5mm, +8mm, +12mm; seven combinations in total). To date, other femoral head sizes have not been recalled and remain on the market.

Speculations with respect to the influence of taper stiffness - resulting from the lower E-modulus of the material and the taper dimensions - on the observed failure scenarios have been made [20], but have not yet been systematically investigated. Furthermore, the role of tip clearance (TC), in the progression of GTF is not fully understood. The TC is defined as the axial distance of the tip of the male stem taper and the bottom of the female head taper. If the female head taper is widened by material loss due to corrosion, the stem taper sinks deeper into the head until the TC is reduced to zero and the tip of the stem taper and the bottom of the head taper get in contact. This process is called bottoming out. In this situation, the force-locking of the taper junction has failed and the head is no longer prevented from spinning on the stem taper when a torque around the taper axis is applied to it. Such a torque always occurs during joint movement due to the friction in the joint articulation [21]. Gross stem taper

failure (GTF) is the final failure mode after bottoming out, whereby the stem taper has been abrasively worn down by the spinning head to such an extent that the head can easily disassociate from the stem. Hence, the purpose of this study was (i) to investigate the time course of the head and stem taper material loss for the particular implant combination based on retrieved components, to (ii) analytically estimate the original tip clearance for these components and (iii) to investigate the general influence of material characteristics and taper size on relative motions at the head-stem-taper interface based on numerical modelling.

Material and Methods

Explant analysis

A total of 30 retrieved CoCr metal heads articulating against PE were available for analysis (LFIT Anatomic heads, Stryker, Mahwah, NJ). For 10 of these heads, the stems made of TMZF-Titanium alloy with a V-40 taper were also available (Accolade I stems, both Stryker, Mahwah, NJ). All these stems were from GTF cases with disassociation (n=9) or disassociation and fracture (n=1) (Figure 2). Clinical data were limited to time-in-situ, patient gender and age (Table 1). To our knowledge, the remaining 20 other stems were left in the patient during revision.

To determine material loss, the female head tapers were scanned with a tactile coordinate measuring machine (Mitutoyo BHN 805, Tokyo, Japan; ruby sphere diameter: 2 mm; 3 µm precision; scanning grid 0.1 mm x 0.1 mm). Since the original geometry of the taper was unknown due to the manufacturing tolerances, it was estimated for each implant individually by a least square fit reconstruction of a global, regular reference from the original surface excluding the worn areas [22]. Female taper material loss volume was calculated as the difference between the reconstructed and the worn geometry. Taper angles and diameters were determined from the reconstructed geometry. Retrieved heads were grouped according to whether they showed signs of bottoming out (defined as wear at the base of the female head taper indicating contact with the tip of the male stem taper; “bottoming out” group) or not (“wear only “ group).

The neck and taper surfaces of the retrieved male stems were scanned using a structured-light 3D scanner (Artec Spider, Artec3D, Luxembourg; 100µm resolution; 50µm point accuracy). Post-processing of the resulting 3D point clouds was conducted in Artec Studio 12 (Professional; Artec3D, Luxembourg). Conversion to a stereolithograph (STL) output rendered a closed triangulated mesh representation of the three dimensional surface of the stems from which the total neck and taper volume was

calculated. The accuracy of this approach was determined by calculating the volume of a solid cube (size: 28 x 28 x 28mm) from the resulting scanned STL surface and comparing this to the volume calculated from the weight and density of the cube (material: AW2007; density: 2850 kg/m³; weight: 62.0g). The accuracy of the scanning method was found to be above 98.1%.

Due to the extent of damage (Figure 2), the original geometry (and hence, original volume) of the neck and taper of the GTF stems could not be estimated from the scanned dimensions. Pristine stems of similar size and neck length were scanned, and the neck and taper volumes were calculated using the same approach as for the retrieved stems. Not all pristine sizes were available for comparison since Accolade I stems are no longer on the market. For this reason, the original neck and taper volumes of all GTF stems were estimated based on the volume of the respective four available stem sizes (3, 4, 5, 8). A linear regression model of stem offset and neck length was fitted to the measured volumes. The correlation coefficient was 0.97 (p=0.18), the mean deviation of the estimated volume from the known volume of the available stem sizes was 2.4% (maximum deviation 3.3%). The total material loss of the stem was calculated as the difference between the estimated original volumes and the measured (scanned) volumes (Figure 3).

Analytical determination of the tip clearance

The initial tip clearance for an assembly force of 0N was determined for the geometries of pristine (n=3) and retrieved (n=16) LFIT V40 CoCr heads, which had been implanted with Rejuvenate or Accolade stems and still exhibited sufficient taper area without material loss. Head diameters were in the range of 36 mm to 44 mm, and head length in the range from -5 mm to +10 mm. The averaged geometry of an Accolade I TMZF V40 stem taper was determined from the four aforementioned pristine stems available, using the same **t**actile coordinate measuring approach and subsequent least square fit algorithm as described above. Each of the 19 heads was combined with this averaged stem taper geometry.

All head-stem combinations showed a positive taper angle difference between female and male taper, which is indicative of a proximal taper engagement (α_{female}-$\alpha_{male} > 0$; Figure 4). The tip clearance was determined with an analytical model using equation 1.

$$TC = \frac{dia_{prox,male} - dia_{prox,female}}{2 * \tan(\alpha_{female}/2)} \qquad \text{Equation 1}$$

whereby $dia_{prox,male}$ and $dia_{prox,female}$ are the proximal diameters of the male and female tapers respectively (Figure 4).

Numerical determination of the micromotion at the taper interface

To investigate the influence of taper material and size on micromotions between head and stem tapers, a simple Finite Element Model (FEM) was constructed (Abaqus/CAE 6.14-2, Dassault Systèmes Simulia Corp., Providence, RI, USA; Figure 5). Element size was chosen based on a convergence study. Four different stem taper materials (CoCr, 316L, Ti6Al4V and TMZF; Table 2) were combined with three idealized taper geometries representing taper designs of *11/13*, *12/14* and *14/16* (male proximal diameters of 11.5 mm, 12.5 mm and 14.5 mm with a male taper length of 15 mm). The 11/13 taper resembles the V-40 taper design. Element sizes were chosen based on a convergence study (Table 3). Corresponding male taper angles were chosen to be 0.04° smaller to achieve a defined proximal taper contact situation [23] (Figure 4). The stem geometries are idealized to represent standard taper dimensions without matching a specific manufacturer's design. In all cases, a CoCr head with an outer diameter of 36 mm was modelled.

The numerical simulation was of a simplified loading situation in the hip joint (Figure 5). The distal end of the stem taper was fixed. After achieving contact of the taper surfaces in an initiation step, the head was subsequently impacted with an axial load of 4kN in the direction of the taper axis in an assembly and seating step. This load was found to provide sufficient fixation strength to prevent head loosening on the stem taper during activities [24]. This was followed by the application of a simplified joint force of 2kN at an angle of 33° to the taper axis, pointing towards the rotational center of the head (Figure 5); the loading was chosen based on the ASTM F2345 standard. For all combinations (4 materials x 3 sizes) the taper deformation, as well as the micromotion at the taper contact area due to a simplified joint force application, were determined (Figure 5). Micromotions are defined as the relative motion between the contacting female and taper surfaces following loading. Micromotion values are reported for the distal edge of the taper contact area after assembly since this is where the largest micromotions occur during loading.

Statistics

Statistical analysis was conducted using Regression and Analysis of variance procedures for normally distributed data and Kruskal-Wallis test for not normally distributed data. The probability of a Type I error was set to 5%. Bootstrapping was used to estimate the distribution of the sampling population (IBM SPSS Statistics 22, Armonk, New York, USA).

Results

The material loss at the head taper increases with time in situ (r^2=0.50, p<0.001; Figure 6). Head length showed a slight tendency to increase the head taper material loss rate (p=0.14; Table 4). The heads in the "bottoming out" group (n=12) tended to be longer, showed higher material loss, higher maximal wear depth and were in-situ for a longer time compared to the heads in the "wear only" group (Table 4, Figure 6, Figure 7). The heads from stems with GTF all belonged to the "bottoming out" group and exhibited wear volumes of above 15mm³. They showed either a "Bird Beak", a "Toothpick" (n=1) or a "Trumpet" (n=1) material loss pattern, dependent on head length (Figure 8). The taper with the "Trumpet" material loss pattern had failed by fracture at the most distal contact point between head and stem (Figure 2, Figure 8). Each material loss pattern had characteristic wear marks at the base of the head taper and at the tip of the stem taper associated with it (Figure 8). All heads of the "bottoming out" group showed circumferential wear tracks at the female taper surface, indicating spinning of the heads on the stem tapers (Figure 7, Figure 8). Stem wear for the GTF group was large with large variations (713.6mm³, SD 252.3mm³) but did not show an influence of the time in situ (Figure 6; p=0.714) or of any other design parameter (Table 1).

The mean tip clearance determined with the analytical model was 1.53 mm (SD: 0.11 mm). No differences in tip clearance were seen between the different head sizes (p = 0.331) or head length (p = 0.144). A mean circumferential radial material loss in the head taper greater than 76 µm (SD: 11 µm) was estimated to be sufficient to result in zero tip clearance and cause bottoming out.

The numerical model showed smaller taper deformations due to the joint force application for larger taper diameters and stiffer materials (Figure 9 left). The micromotion at the distal edge of the taper contact area due to joint load application showed very large differences between the four materials and large differences between the three taper sizes (Figure 9 right). The statistical analysis comparing the taper sizes for all materials combined revealed no significant differences between the taper sizes (deformation: p=0.19, micromotion: p=0.729; Figure 9). The analysis comparing materials for all taper sizes combined, however, revealed significant differences between the materials. The deformation and

the micromotion was significantly larger for the TMZF-alloy compared to the CoCr-alloy (deformation: TMZF: 33.1+/-11.1µm vs. CoCr 12.9+/-4.2µm, p=0.03; micromotion: TMZF 2.2+/- 0.27µm vs. CoCr 1.3+/-0.06µm, p< 0.001; Figure 9). The Ti6Al4V-alloy exhibited a similar result in comparison to the CoCr- and the 316L-alloys, but the differences were not statistically significant (Figure 9).

In addition to the increased magnitude, a different micromotion pattern between head and stem for the Ti6Al4V- and TMZF-alloys compared to the CoCr-alloy and the 316L-alloy was found (Figure 10). Whereas maximum micromotion for the two less stiff Ti-alloys occurs on the taper side away from the joint force (counter-clockwise tilting of the head on the taper), for the two stiffer materials it occurs on the side on which the force is applied (clockwise tilting of the head on the taper). These differences are caused by the differences in stem taper deformation between the four materials.

Discussion

The most important result of the retrieval study was that the analysed 36mm CoCr heads exhibited major material loss of the female head taper due to fretting and corrosion, which increased with time in situ. None of the other design specific parameters investigated showed a significant influence on the amount of material loss, only the head length showed a trend to increase material loss (Table 4). It has to be noted that all analyzed stems had a CCD angle of 127°, none of the GTF cases had a CCD angle of 132°, which was also available. This missing correlation corresponds to the results for the material loss of CoCr neck pieces from Rejuvenate stems (Stryker, Mahwah, NJ), which are made from the same TMZF-alloy as the Accolade I stem [25]. Material loss of the CoCr female head taper increased by about 2.7mm³ for every year in situ, with bottoming out to occur with a material loss of 15 mm³ and above (Figure 6). Bottoming out of the head occurred in 12 of the 30 cases. At first sight it may seem surprising that the harder CoCr head taper in contact with the softer Ti-alloy stem is exposed to material loss, whereas the stem taper initially stays rather undamaged. However, this phenomenon is reported in the literature as ‘imprinting’ by several authors [26;27]. The reason for it is that oxidized titanium has a significantly higher hardness value, therefore damaging the unoxidized cobalt-chrome material [28]. After the widening of the female taper results in bottoming out, the mechanism for material loss changes: from corrosion to abrasion causing the softer Titanium to wear down.

The three observed GTF patterns “Bird Beak, “Toothpick” and “Trumpet” were directly related to the length of the head, which determines the position of the stem taper center with respect to the head center and thus the associated dominant moment direction caused by the hip joint load axis (Figure

11). The resulting stresses at the taper interface [20;29] cause varus or valgus tilting of the head (Figure 11). It should be noted that the “Toothpick” and “Trumpet” damage patterns have not yet been reported elsewhere and were only observed in one sample each. A further contributing factor is the accelerated corrosion of TMZF in simulated body fluid in comparison to Ti6Al4V, which might further precipitate the process [30]. It is surprising that the catastrophic GTF cases did apparently not exhibit clinical symptoms due to raised Co and Cr metal ions, which must have been caused by the amount of CoCr lost from the female head taper (above 15mm³, Figure 6, Figure 7), and/or the large amounts of TMZF abraded from the male stem taper. A possible explanation could be that only a relatively small amount of female taper widening is required before the tip clearance is minimized and bottoming out occurs. The estimated value of 76 µm (SD: 11 µm) lies well within the observed wear depth determined for the GTF cases. After bottoming out, material loss is dominantly caused by abrasion of the spinning head on the damaged taper rather than corrosion. It could be speculated, that abrasive CoCr debris might have a different particle size, causing a different biological reaction compared to corrosion debris. The overall frequency of the GTF phenomenon in THA seems to be rather low. Gross Taper Failure of stems that are not made from TMZF-alloy are reported in the literature for only three cases. The stems of these failures were all made from standard Ti-6Al-4V titanium: one failure of a small 6° 10/12 taper of a titanium-alloy porous-coated Harris hip stem after 14 years in situ in an active working farmer [31], one failure of a skirted head on a Bimetric Stem with a type I taper in a patient with a BMI of 30 after 8 years [16], and one failure for a ML extended offset 12/14 taper stem in a patient with a BMI of 40 after 8 years [16]. This indicates that GTF is not totally limited to TMZF stems with a V40 taper, even so the extend is much larger [9-18].

The results of the Finite Element Model show that the micromotion at the head-stem taper interface is largest for the tapers made from TMZF-alloy, followed by Ti6Al4V-alloy, which also exhibited an elevated micromotion compared to the two stiffer taper materials. These differences could explain why the GTF phenomenon is mostly reported for stems made of TMZF-alloy and for a few cases for stems made from Ti6Al4V-alloy, but not for stems made from CoCr or 316L. The numerical results indicate that the material has a stronger influence than the taper size. Taper size showed an increased micromotion for smaller tapers, but the increase was not as pronounced as the differences between the four materials. The largest micromotions were found for the 11/13 taper made from TMZF-alloy, which further supports the suggestion that this combination is more susceptible to extensive wear and

GTF problems. The significance of the different movement patterns between the materials is not yet understood but will be further investigated.

For the particular Accolade I stem design with a V-40 taper, reports for good clinical performance (without mentioning head size) are reported in the literature [32;33]. The Orthopaedic Data Evaluation Panel ODEP of UK and Wales lists an ODEP rating of 10A* for the Accolade-I stem in 2017, i.e. the best rating awarded by the ODEP, which indicates that the 10-year revision rate lies below 5% (http://www.odep.org.uk/products.aspx) . These reports indicate that there is no "general" problem with the specific design itself, but rather that the problems might be caused in combination with adverse factors such has high loading or large head sizes [1;20]. This might also explain, why these problems are not reported in Europe since here the head diameter used against Polyethylene is predominantly 28 or 32mm. The widespread use of ceramic heads might have further helped to keep the problem small in Europe [34]. The Accolade I stem was never recalled, but in 2012 replaced with the Accolade-II stem made from standard Ti-6Al-4V titanium alloy. The use of the Accolade I stem consequently declined rapidly: the 2017 Annual Report of the Australian Joint Registry lists for the year 2013 the use of 765 Accolade I stems. For 2014 the Accolade I stem is absent from the list of the 10 most used uncemented stems, and replaced by the Accolade II stem with 523 implantations. In this context, it has to be highlighted that more than 50% of the CoCr heads analysed in this study do not belong to the recalled sizes. This is a similar finding to other authors [14] and further highlights that not only one adverse combination of several factors is able to initiate the corrosion process.

The study has several limitations. No patient-specific information was available. It would have been very interesting to determine the influence of patient BMI and level of activity on the magnitude of material loss. However in an earlier study assessing the material loss of CoCr neck pieces from Rejuvenate stems, which are made from the same TMZF-alloy as the Accolade I stem, this information was available but did not yield any additional insight [25]. For the pristine heads, tip clearance could only be estimated for non-recalled sizes since no retrieved heads of the recalled size could be obtained. The analytical model also does not consider chamfers or the relief groove and the tip clearance had to be estimated for an assembly without assembly force. The determined value corresponds to a best case scenario since the intra-operatively achieved tip clearance after seating the head with a hammer stroke will be even lower than the value determined with the model. The amount of stem wear of the GTF cases could not be determined directly since original stems are no longer

available. This, however, should not influence the results greatly since the chosen approximation approach was shown to produce only minor deviations for known original stem geometries, but the values should only be viewed as a rough estimate. This is the first time that an attempt is made to give a quantitative approximation of the stem taper material loss. Consequently, no comparison to literature values was possible. Finally, in-vivo assembly and loading have a high variability. In this study only one defined loading and assembly situation was modeled in the FEM analysis. Higher loading and sub-optimal assembly might further increase the determined micromotions.

Conclusions

Follow-up examinations of patients treated with the respective stem type in combination with large CoCr heads should include metal ion determination in blood or serum, even if no clinical symptoms are present. This might allow the detection of taper corrosion before catastrophic failure of the taper connection occurs. Testing should not be solely restricted to patients that were treated with heads sizes that have been recalled since many of the failed cases analysed belong to heads not included in the recall. Deformation and micromotion were shown to occur for all combinations of taper size and taper material. As a consequence, taper assembly should be optimized and taper bending load - where possible – minimized, even if larger tapers and stiffer materials are utilized. These reduce the risk of micromotion but do not fully eliminate it. The higher micromotion shown for small tapers made from less stiff materials should be used as a basis for future designs, acknowledging that an absolute limit for critical micromotion is not known.

Acknowledgement

The research has received funding from the European Union's Seventh Frame-work Program (FP7/2007-2013) under grant agreement no. GA-310477 LifeLongJoints.

References

1. Morlock MM: The taper disaster - how could it happen? Hip Int 25(4):339, 2015
2. Cooper HJ, la Valle CJ, Berger RA, Tetreault M, Paprosky WG, Sporer SM, Jacobs JJ: Corrosion at the head-neck taper as a cause for adverse local tissue reactions after total hip arthroplasty. J Bone Joint Surg Am 94(18):1655, 2012
3. McGrory BJ, MacKenzie J, Babikian G: A High Prevalence of Corrosion at the Head-Neck Taper with Contemporary Zimmer Non-Cemented Femoral Hip Components. J Arthroplasty 30(7):1265, 2015
4. Goldberg JR, Gilbert JL, Jacobs JJ, Bauer TW, Paprosky W, Leurgans S: A multicenter retrieval study of the taper interfaces of modular hip prostheses. Clin Orthop Relat Res(401):149, 2002
5. Gilbert JL, Buckley CA, Jacobs JJ: In vivo corrosion of modular hip prosthesis components in mixed and similar metal combinations. The effect of crevice, stress, motion, and alloy coupling. J Biomed Mater Res 27(12):1533, 1993
6. Porter DA, Urban RM, Jacobs JJ, Gilbert JL, Rodriguez JA, Cooper HJ: Modern trunnions are more flexible: a mechanical analysis of THA taper designs. Clin Orthop Relat Res 472(12):3963, 2014
7. Krull A, Morlock MM, Bishop NE: The Influence of Contamination and Cleaning on the Strength of Modular Head Taper Fixation in Total Hip Arthroplasty. J Arthroplasty 32(10):3200, 2017
8. Jauch SY, Huber G, Sellenschloh K, Haschke H, Baxmann M, Grupp TM, Morlock MM: Micromotions at the taper interface between stem and neck adapter of a bimodular hip prosthesis during activities of daily living. J Orthop Res 31(8):1165, 2013
9. Craig P, Bancroft G, Burton A, Collier S, Shaylor P, Sinha A: Raised levels of metal ions in the blood in patients who have undergone uncemented metal-on-polyethylene Trident-Accolade total hip replacement. Bone Joint J 96-B(1):43, 2014
10. Spanyer J, Hines J, Beaumont CM, Yerasimides J: Catastrophic Femoral Neck Failure after THA with the Accolade((R)) I Stem in Three Patients. Clin Orthop Relat Res 474(5):1333, 2016
11. Patel S, Talmo CT, Nandi S: Head-neck taper corrosion following total hip arthroplasty with Stryker Meridian stem. Hip Int 26(6):e49-e51, 2016
12. Swann RP, Webb JE, Cass JR, Van Citters DW, Lewallen DG: Catastrophic Head-Neck Dissociation of a Modular Cementless Femoral Component. JBJS Case Connect 5(3):e71, 2015
13. Raju S, Chinnakkannu K, Puttaswamy MK, Phillips MJ: Trunnion Corrosion in Metal-on-Polyethylene Total Hip Arthroplasty: A Case Series. J Am Acad Orthop Surg 25(2):133, 2017

14. Urish KL, Hamlin BR, Plakseychuk AY, Levison TJ, Higgs GB, Kurtz SM, DiGioia AM: Trunnion Failure of the Recalled Low Friction Ion Treatment Cobalt Chromium Alloy Femoral Head. J Arthroplasty 32(9):2857, 2017
15. Ko L, Chen A, Deirmengian G, Hozack W, Sharkey P. Catastrophic Femoral Head-Stem Trunnion Dissociation Secondary to Corrosion. JBJS 98-A, 1400-1404. 2016.
16. Banerjee S, Cherian JJ, Bono JV, Kurtz SM, Geesink R, Meneghini RM, Delanois RE, Mont MA: Gross trunnion failure after primary total hip arthroplasty. J Arthroplasty 30(4):641, 2015
17. Kim WY, Ko MS, Lee SW, Kim KS: Short-term Outcomes of Ceramic Coated Metal-on-Metal Large Head in Total Hip Replacement Arthroplasty. Hip Pelvis 30(1):12, 2018
18. Walker PS, Campbell PA, Brazil D, McTighe T. Trunnion Corrosion and Early Failure in Monolithic Metal-on-Polyethylene TMZF Femoral Components: A case series. Reconstructive Review 6[3], 13-18. 2016.
19. Stryker Osteonics TA. TMZF(R) Alloy: A Titanium Alloy Optimized for Orthopaedic Implants. http://www.stryker.gr/st_pdf_ltmzfb.pdf (Accessed 19/06/2018) . 2018.
20. Morlock M, Bünte D, Gührs J, Bishop N: Corrosion of the Head-Stem Taper Junction - Are We on the Verge of an Epidemic? HSS Journal 13:42, 2017
21. Damm P, Bender A, Bergmann G: Postoperative changes in in vivo measured friction in total hip joint prosthesis during walking. PLoS One 10(3):e0120438, 2015
22. Bishop N, Witt F, Pourzal R, Fischer A, Rutschi M, Michel M, Morlock M: Wear patterns of taper connections in retrieved large diameter metal-on-metal bearings. J Orthop Res 31(7):1116, 2013
23. Mueller U, Panzram B, Braun S, Sonntag R, Kretzer JP: Mixing of Head-Stem Components in Total Hip Arthroplasty. J Arthroplasty 33(3):945, 2018
24. Rehmer A, Bishop NE, Morlock MM: Influence of assembly procedure and material combination on the strength of the taper connection at the head-neck junction of modular hip endoprostheses. Clin Biomech (Bristol , Avon) 27(1):77, 2012
25. Buente D, Huber G, Bishop N, Morlock M: Quantification of material loss from the neck piece taper junctions of a bimodular primary hip prosthesis. A retrieval study from 27 failed Rejuvenate bimodular hip arthroplasties. Bone Joint J 97-B(10):1350, 2015
26. Bishop N, Witt F, Pourzal R, Fischer A, Rutschi M, Michel M, Morlock M: Wear patterns of taper connections in retrieved large diameter metal-on-metal bearings. J Orthop Res 31(7):1116, 2013

27. Arnholt CM, Macdonald DW, Underwood RJ, Guyer EP, Rimnac CM, Kurtz SM, Mont MA, Klein GR, Lee GC, Chen AF, Hamlin BR, Cates HE, Malkani AL, Kraay MJ: Do Stem Taper Microgrooves Influence Taper Corrosion in Total Hip Arthroplasty? A Matched Cohort Retrieval Study. J Arthroplasty 32(4):1363, 2017
28. Moharrami N, Langton DJ, Sayginer O, Bull SJ. Why does titanium alloy wear cobalt chrome alloy despite lower bulk hardness: A nanoindentation study? Thin Solid Films [549], 79-86. 2013.
29. Bishop NE, Burton A, Maheson M, Morlock MM: Biomechanics of short hip endoprostheses--the risk of bone failure increases with decreasing implant size. Clin Biomech (Bristol , Avon) 25(7):666, 2010
30. Yang X, Hutchinson CR: Corrosion-wear of beta-Ti alloy TMZF (Ti-12Mo-6Zr-2Fe) in simulated body fluid. Acta Biomater 42:429, 2016
31. Arvinte D, Kiran M, Sood M. Femoral Head-Trunnion Dissociation Secondary to Corrosion of a Modular Total Hip Replacement. JBJS Case Connect 5[2], e35. 2015.
32. Pierce TP, Jauregui JJ, Cherian JJ, Elmallah RD, Robinson K, Mont MA: Prospective evaluation of short and mid-term outcomes of total hip arthroplasty using the Accolade stem. Hip Int 25(5):447, 2015
33. Casper DS, Kim GK, Restrepo C, Parvizi J, Rothman RH: Primary total hip arthroplasty with an uncemented femoral component five- to nine-year results. J Arthroplasty 26(6):838, 2011
34. Kurtz SM, Kocagoz SB, Hanzlik JA, Underwood RJ, Gilbert JL, Macdonald DW, Lee GC, Mont MA, Kraay MJ, Klein GR, Parvizi J, Rimnac CM: Do ceramic femoral heads reduce taper fretting corrosion in hip arthroplasty? A retrieval study. Clin Orthop Relat Res 471(10):3270, 2013

Tables

Table 1: Patient and implant data of the retrieved implant components. All stems had a neck angle of 127° (Group: 1, wear only, no stem available; Group 2: bottoming out; failure patterns are explained in Figures 8&10; components which have not been recalled have been marked by grey background).

Table 2: Properties of the materials investigated.

Table 3: Specifications of the FE-Model.

Table 4: Patient, implant and material loss data for the two groups (p-values represent the comparison for each variable between the 2 groups; SD: Standard Deviation).

Table 5: Maximum deformation of the male taper due to loading [µm].

Table 1: Patient and implant data of the retrieved implant components. Components which have not been recalled are marked by grey background. All analyzed stems had a neck angle of 127° (Group: 1, wear only, no stem available; Group 2: bottoming out; failure patterns are explained in Figures 8 and 10;).

Nr	Group (failure pattern)	Sex	Age at Implantation	Time in situ [years]	Stem Size	Stem length [mm]	Neck length [mm]	Offset [mm]	Head dia-meter [mm]	Head length [mm]
1	1	F	70	3,3					36	**-5**
2	1	M	70	6,0					40	**0**
3	1	F	33	7,1					32	**4**
4	1	M	67	6,4					44	**0**
5	1	F	62	3,9					44	**-4**
6	1	F	58	6,2					40	**-4**
7	1	F	64	3,1					36	5
8	1	F	32	7,0					32	**4**
9	1	M	53	1,9					36	**0**
10	1	M	53	5,3					32	**0**
11	1	F	55	3,6					36	**0**
12	1	M	69	4,8					36	**0**
13	1	F	82	4,6					36	**-5**
14	1	F	59	4,9					44	**0**
15	1	M	62	7,4					36	5
16	1	F	59	6,7					40	**4**
17	1	F	69	3,8					36	**10**
18	1	M	72	1,3					36	5
19	2, no stem	F	50	6,3					36	5
20	2, no stem	F	70	7,2					36	5
21	2, (bird beak)	F	85	9,7	1,0	110,0	30,0	38,0	36	5
22	2, (bird beak)	M	65	6,2	3,0	120,0	35,0	43,0	36	5
23	2, (toothpick)	M	52	10,7	3,0	120,0	35,0	43,0	36	**0**
24	2, (bird beak)	M	52	8,3	3,5	124,0	35,0	43,0	36	5
25	2, (bird beak)	M	70	9,8	4,5	129,0	35,0	45,0	36	5
26	2, (bird beak)	M	74	8,3	5,0	130,0	37,0	48,0	36	5
27	2, (trumpet)	M	51	6,5	5,0	130,0	37,0	48,0	36	**-5**
28	2, (bird beak)	M	55	7,7	5,0	130,0	37,0	48,0	36	5
29	2, (bird beak)	M	78	9,2	5,5	133,0	37,0	49,0	36	5
30	2, (bird beak)	M	71	5,8	5,5	133,0	37,0	49,0	36	5

425

426 Table 2: Properties of the materials investigated.

Material	Modulus [GPa]	Poisson's ratio [1]
Co28Cr6Mo	220.0	0.29
316L	200.0	0.28
Ti6Al4V	110.0	0.32
Ti12Mo6Zr2Fe (TMZF)	79.5	0.33

427

428 Table 3: Specifications of the FE-Model.

Element type	C3D8R
Element size of meshed contact area (head/taper)	0.6 mm / 0.3 mm
Number of elements stem taper (11/13, 12/14, 14/16)	111488 / 128908 / 171520
Numb. of elements head taper (11/13, 12/14, 14/16)	28022 / 28514 / 28635
Friction coefficient between head and stem for all combinations	0.3

429

430 Table 4: Patient, implant and material loss data for the two groups (p-values represent the
431 comparison for each variable between the 2 groups; SD: Standard Deviation).

Group	n [#]	Age [years]	SD	Time in situ [years]	SD	Head length [cm]	SD	Head diameter [mm]	SD	Max Wear depth [µm]	SD	Material loss [mm³]	SD
wear only	18	60.5	12.6	4.9	1.8	1.1	4.1	37.3	3.9	60.4	25.8	5.1	4.0
bottoming out	12	64.4	12.0	8.0	1.6	3.8	3.1	36.0	0.0	148.6	47.5	20.8	3.6
p-value		n.s. p=0.403		sig. p<0.001		n.s. p=0.063		n.s. p=0.247		sig. p<0.001		sig. p<0.001	

432

433

434 Table 5: Maximum deformation of the male taper due to loading [µm].

Taper Size	TMZF	Ti6Al4V	316L	CoCr
11/13	43.7	32.2	18.4	16.8
12/14	34.1	25.3	14.6	13.4
14/16	21.6	16.0	9.3	8.5

435

436

Figure Legends

Figure 1: Gross Taper Failure of an Accolade I stem after more than 10.5 years in the patient (implant #30 in Table 1).

Figure 2: The 10 stems with Gross Taper Failure (from left to right stems #21-30 in Table 1).

Figure 3: Method for the determination of the material loss on the stem neck and taper. Left: The pristine stem of the same size and geometry as the retrieved stem. Middle left: the retrieved damaged stem. Middle right: the 3D reconstruction of the retrieved damaged stem. Right: Difference between pristine and damaged stem (i.e. material loss) is indicated in red.

Figure 4: The geometrical parameters of the taper junction for the determination of tip clearance and contact area. The sketch is greatly exaggerated for easier understanding. The order of magnitude of the real taper angle difference between the male and female tapers is about 0.04°.

Figure 5: Left: The Finite Element Model (Tables 2 and 3) ;
Right: The boundary conditions for the head loading step after assembly.

Figure 6: Material loss of the female and male tapers of the different groups together with the time in situ of the implants (female taper material loss = $-4.9mm^3 + 2.7mm^3$*time_in_situ., $r^2=0.05$, $p<0.001$).

Figure 7: Female head taper material loss patterns ranging from small (left) to very large wear amounts (right). The left 3 images are from heads in group 1 (no bottoming out), the right 2 images from group 2 (bottoming out; first: tooth pick, second: bird beak).

Figure 8: The three observed Gross Taper Failure patterns of the stem (bottom row) were all associated with bottoming out of the male stem taper in the female head taper. Associated with each failure pattern was a specific wear pattern of the tip of the male stem taper (middle row) and the bottom of the female head (top row): “Bird Beak” (left column), “Toothpick” (middle column), “Trumpet” (right column).

Figure 9: left: Maximum stem taper deformation due to loading for the different stem taper materials and sizes.
right: Maximum micromotion at the distal edge of the taper contact due to loading for the different stem taper materials and sizes.

Figure 10: Micromotion at the taper contact area due to loading (black indicates micromotions above 1.5µm, dark blue the non-contact area).

Figure 11: The three observed material loss patterns of the GTF stems were associated with specific head length: The “Bird Beak” pattern with a long head length (+5mm; left), the “Toothpick” pattern with a neutral head (0mm; middle), and the “Trumpet” pattern with a short head (-5mm; right). The dominant direction of the moment around the taper center due to in-vivo joint loading is indicated. The grey arrow indicates the assembly force direction (F=4000N), the dark red arrow the direction of the joint load (F=2600N). The red lines represent the stresses at the taper interface, the orange lines separation of the head taper from the stem taper (the calculations are explained in detail in [26]).

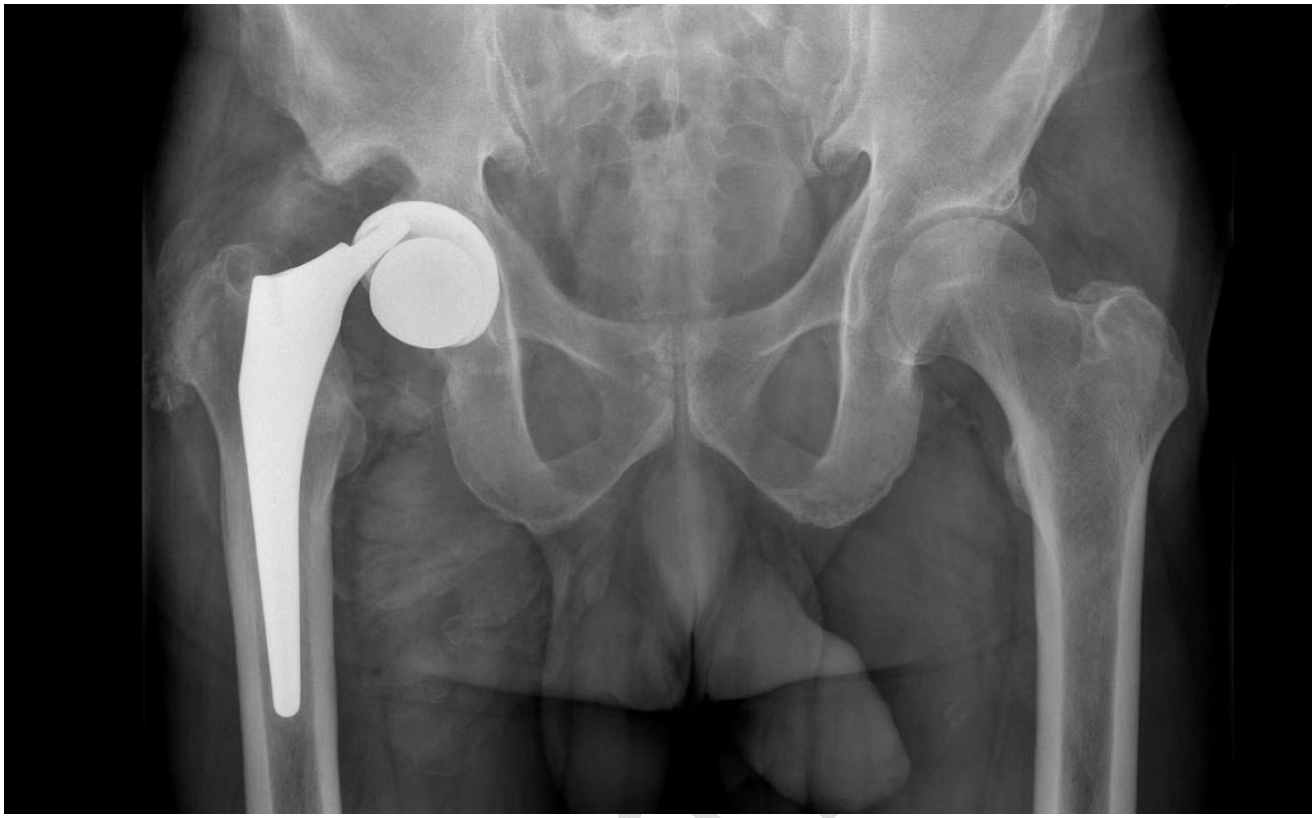

Figure 1

Figure 2

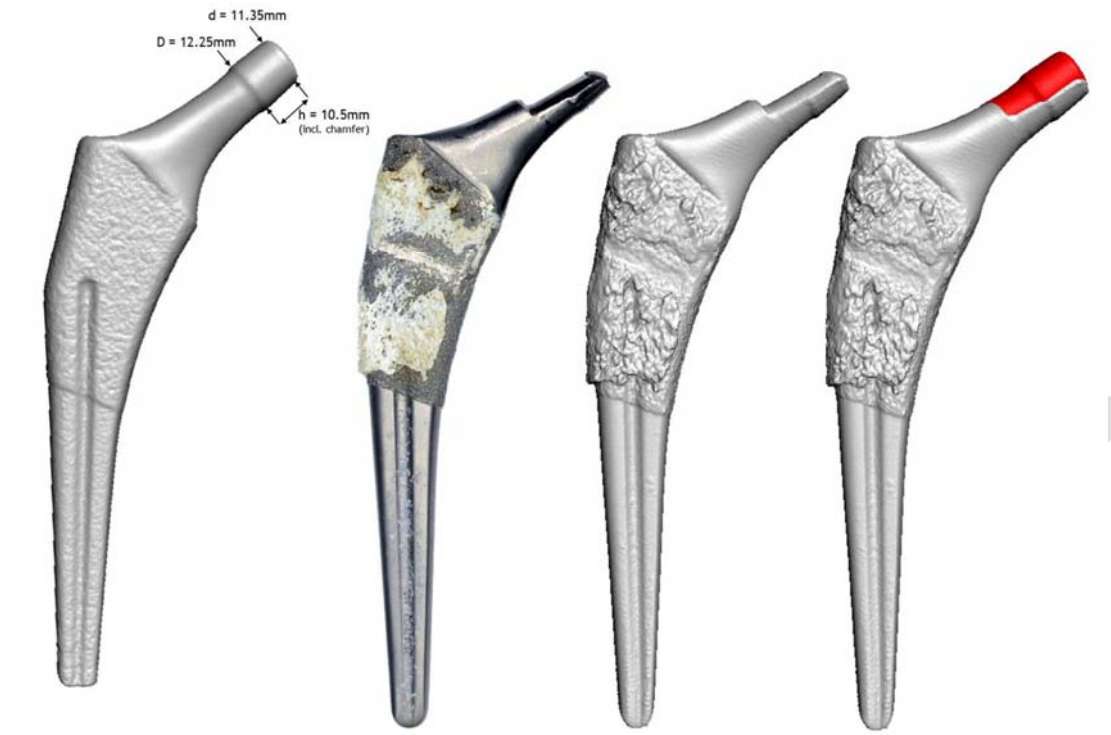

483

484 Figure 3

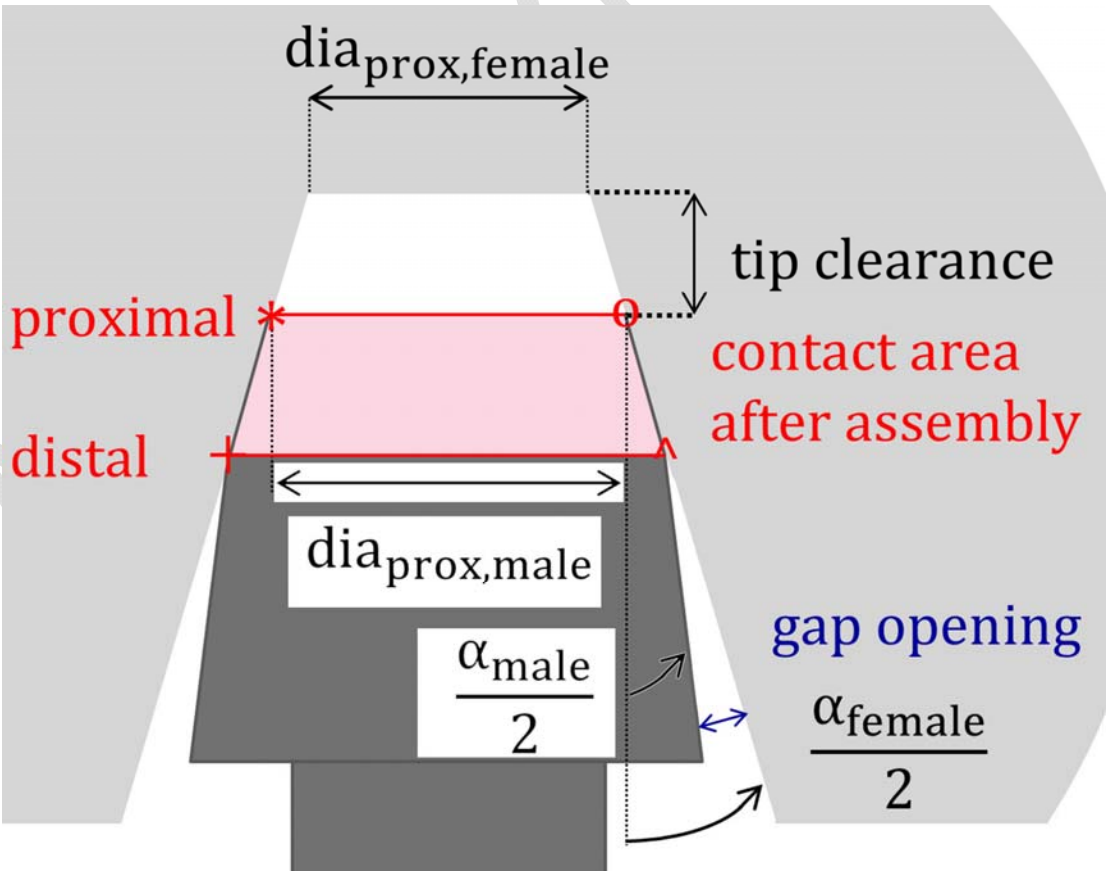

485

486 Figure 4

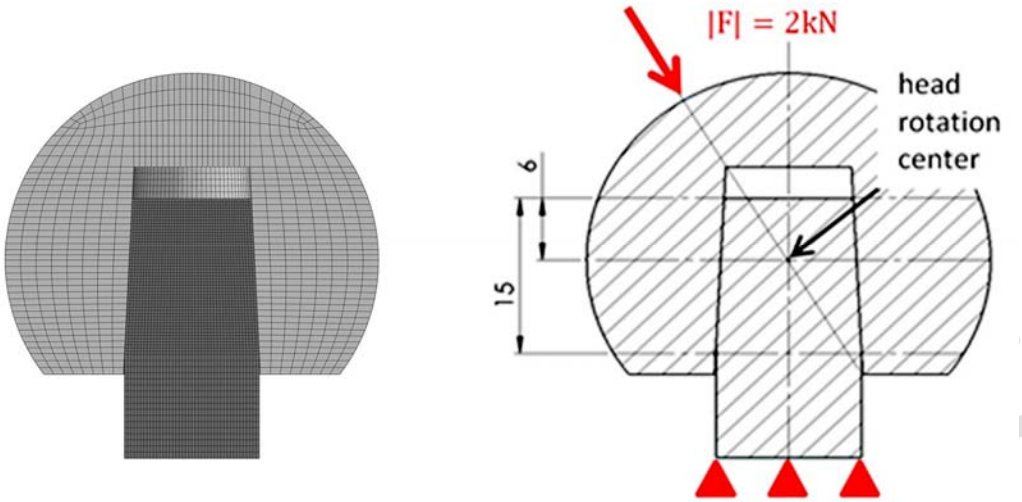

Figure 5

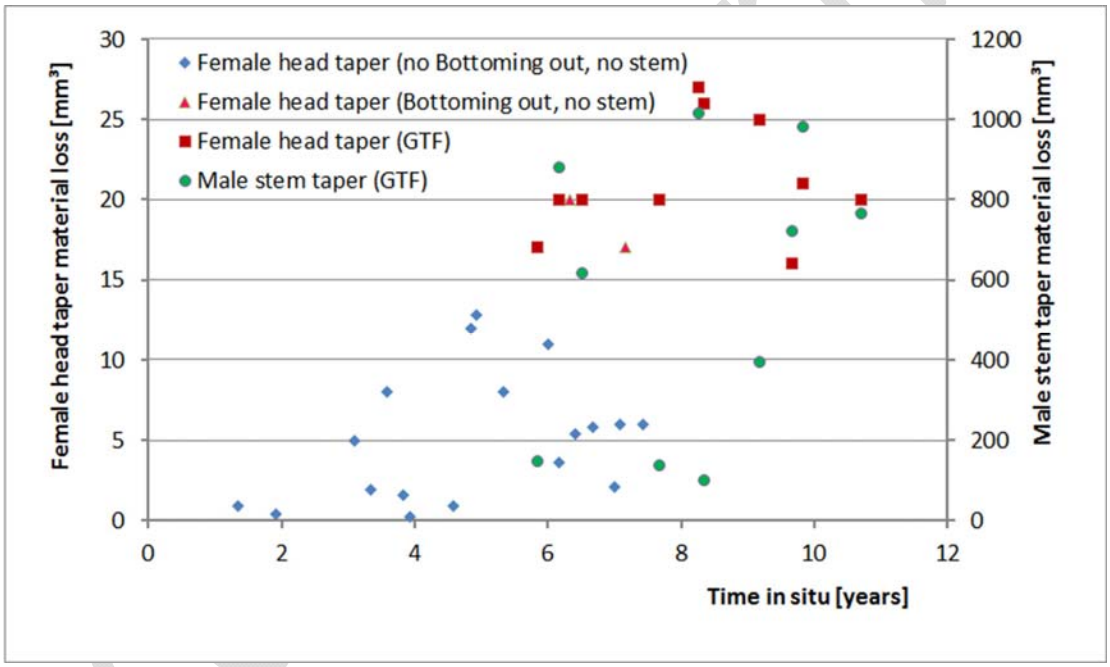

Figure 6

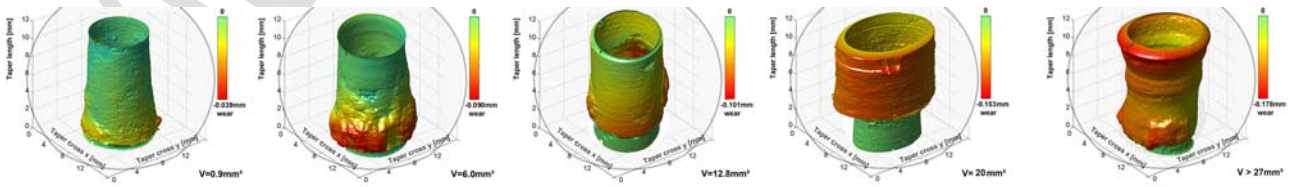

Figure 7

493

494 Figure 8

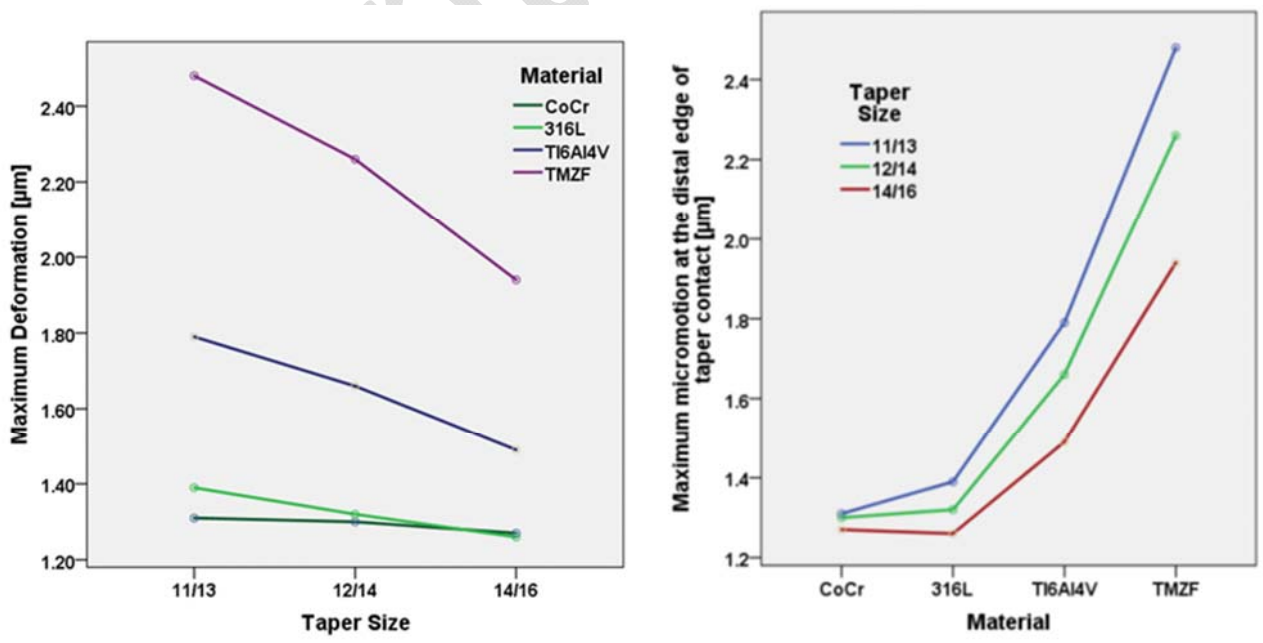

495

496 Figure 9

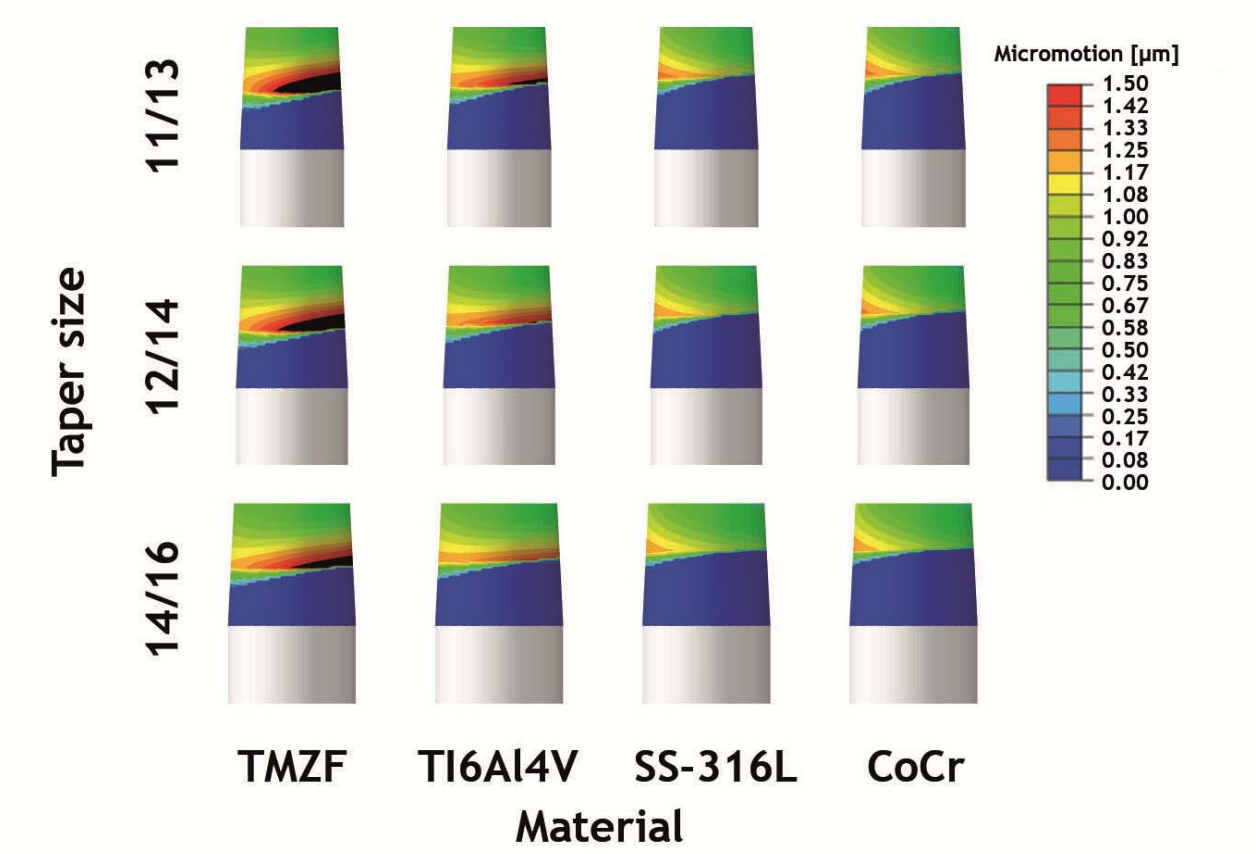

Figure 10

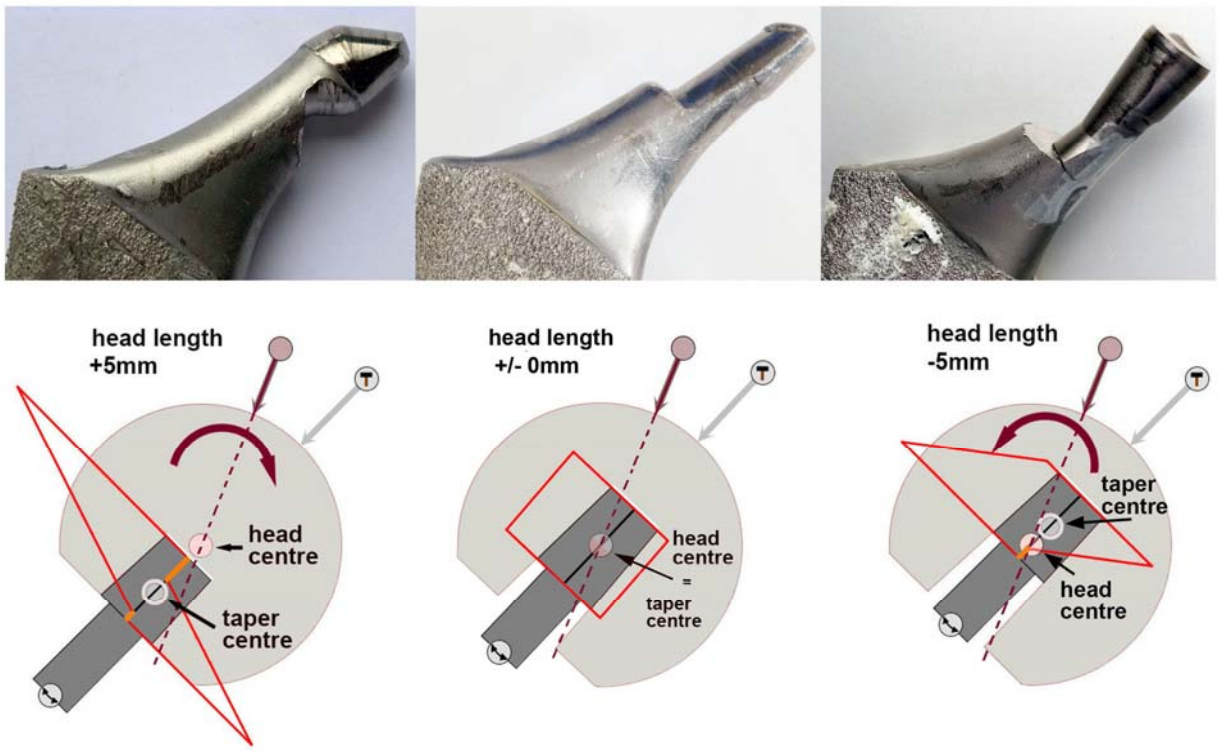

Figure 11